Transactions, SMiRT-25
Charlotte, NC, USA, August 4-9, 2019
Division V

UNCERTAINTY OF DIFFERENT MODELING METHODS OF NPP BUILDING SUBJECT TO SEISMIC GROUND MOTIONS

Byunghyun Choi[1], Akemi Nishida[1], Tadahiko Shiomi[1], Ken Muramatsu[2], and Tsuyoshi Takada[3]

[1] Researcher, Japan Atomic Energy Agency, Chiba, Japan (choi.byunghyun@jaea.go.jp)
[2] Visiting Professor, Tokyo City University, Tokyo, Japan
[3] Professor, The University of Tokyo, Tokyo, Japan

ABSTRACT

In this study, to clarify the influence of the uncertainty of the input seismic ground-motion response of a nuclear power plant (NPP) building, we examined seismic-response analysis results using two different methods of modeling buildings and then compared the results to evaluate effects related to differences between the models. The two methods we used are the three-dimensional (3D) finite-element (FE) model (mainly composed of shell elements) and the conventional sway-rocking (SR) model. Also, using features of the 3D FE model, we analyzed the spatial features of the response results. In this paper, we describe the differences in seismic response obtained by the 3D FE model and the SR model based on simulated input ground motions, and we discuss the influence of the characteristics of the input ground motion on the maximum-response acceleration of the modeled NPP building.

INTRODUCTION

After the 2011 Fukushima accident, nuclear power plants (NPPs) were required to take countermeasures against ground motion beyond basic seismic design, and the importance of seismic probabilistic risk assessment (SPRA) has drawn much attention. In SPRA, uncertainty can be classified into two types: aleatory uncertainty and epistemic uncertainty. To improve the reliability of SPRA, efforts should be made to identify and, if possible, reduce the epistemic uncertainty caused by lack of knowledge. The purpose of this study is to identify epistemic uncertainty caused by methods of modeling NPP buildings. In conventional SPRA, the sway-rocking (SR) model has been regarded as the basic model, because its calculation cost is relatively low, it has been verified with observation records, and most of time it gives conservative results. However, because the SR model is expressed by simplifying a three-dimensional (3D) structure, it includes modeling-related errors. Therefore, to confirm the influence due to modeling differences, we compared SR model results with the response results from detailed 3D finite-element (FE) models. In this paper, we also compare differences between response results by the two modeling methods for each of the input waves. After we link characteristics of each of the input waves and differences in response characteristics caused by the modeling methods, we are able to quantify the difference in seismic response by the two modeling methods. We expected that 3D effects such as out-of-plane deformation of walls and differences due to the position of the same floor, which cannot be expressed by the SR model, can be taken into account by using the 3D FE model,. The obtained knowledge could help SPRA by the quantification of epistemic uncertainty due to differences in seismic-response analysis based on different models.

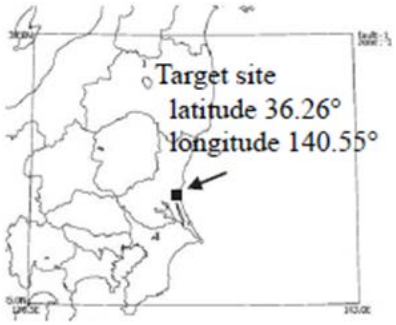

Figure 1. Location of the target site (Nishida et al. 2015a).

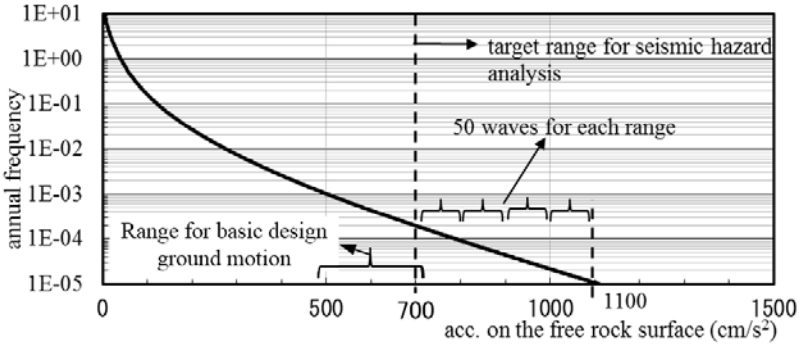

Figure 2. Seismic hazard curve at the target site (Nishida et al. 2015a).

ANALYSIS CONDITIONS

Hazard-Consistent Ground Motions

Ground-motion generation was conducted for the NPP target site in Oarai, Japan (Lat. 36.26°N; Long. 140.55°E) (Figure 1). We evaluated seismic hazard by measuring the intensity of ground motion as the peak ground acceleration (PGA) on a free rock surface, according to the Headquarters for Earthquake Research Promotion （2009). The resulting PGA seismic-hazard curve for the target site is shown in Figure 2. We adopted the attenuation relation proposed by Si and Midorikawa (1999) with the variation of 0.58 for the natural-logarithm standard deviation. For this study, the target range of reproduction of ground motion was selected based on our past research (Nishida et al. 2015a). The target annual exceedance frequency of ground-motion generation is from 10^{-4} to 10^{-5}. Because past SPRA results have shown that core-damage frequencies are about 10^{-5}/year, ground motions with annual exceedance frequencies of 10^{-4} to 10^{-5} would be most influential in evaluations. This range corresponds to PGA in the range 700–1100 cm/s^2 at the NPP site. We divided this range into four intervals (100 cm/s^2 each) and generated 50 ground motions in each interval, producing a total of 200 ground motions within this PGA range. By disaggregation of the seismic-hazard curve, we obtained seismic sources reproducing these motions; we chose the sources according to their contributions to the site hazard by using a stochastic fault-rupture model (Nishida et al. 2015a).

Examples of response spectra and acceleration time-history waveforms generated from different seismic sources are shown in Figure 3, which confirms that the phases of the response spectra are diverse and that the arrival time and the duration of seismic waves vary even for similar hazard levels (1000–1100 cm/s^2). The examples demonstrate that the acceleration waveforms generated by the disaggregation of a hazard curve have advantages over conventional SPRA, for which the variability of the spectrum is not considered, as the shape of the input seismic-motion spectrum is assumed to be the same as the uniform-hazard spectrum or that of the basic earthquake design for the NPP.

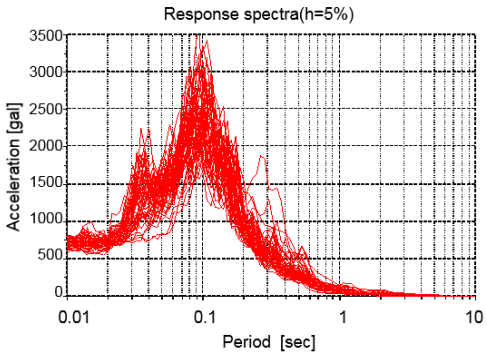

(a) Response spectra (700–800 cm/s^2).

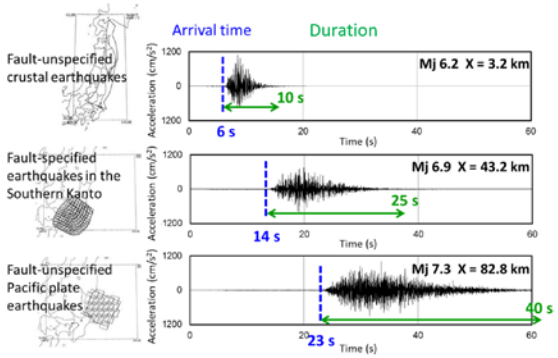

(b) Time-history waveforms (1000–1100 cm/s^2).

Figure 3. Examples of input ground motions from different sources (Nishida et al. 2015a).

Analytical Models and Conditions

We modeled the NPP reactor building in two ways, using a 3D FE model (Figure 4a) with shell elements and using a conventional embedded SR model (Figure 4b). The differences between the two models are quantified as follows. The 3D FE model mainly uses shell elements for the walls and slabs. The number of nodes is ~50,000, and the number of elements is ~60,000. The soil–structure interaction (SSI) is expressed in terms of soil springs (Figure 5). We performed seismic-response analysis using 200 hazard-consistent ground-motion waves by simultaneous excitation in three directions. We used the Rayleigh-damping, direct time-integration, and Newmark-β (β = 1/4 and γ = 1/2) methods in the analysis (Choi et al. 2017). The integration time interval Δt we set to 0.005 s. We used the Maekawa model (Maekawa and Fukuura 1999) for the nonlinear material properties of reinforced concrete. (In contrast, the embedded SR model uses linear materials.)

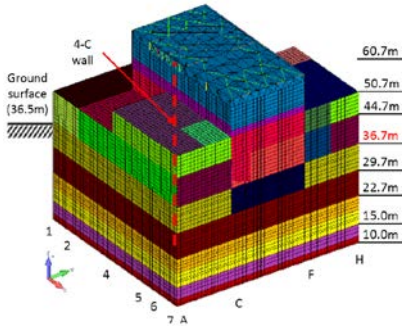

(a) Three-dimensional finite-element model (shell).

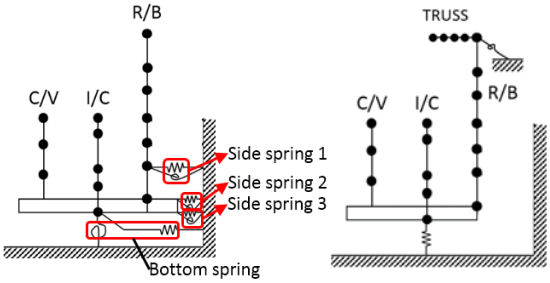

(b) Embedded sway-rocking model (left: horizontal, right: vertical).

Figure 4. Overview of analytical models (Choi et al. 2017).

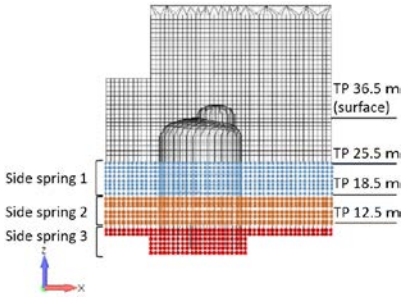

(a) Side springs.

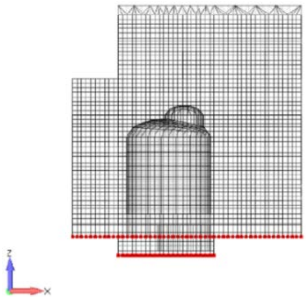

(b) Bottom springs.

Figure 5. Three-dimensional finite-element model's attachment locations of soil springs for soil–structure interaction (Choi et al. 2017).

In the following discussion, we consider the uncertainty of input ground motions to be aleatory uncertainty. (However, we do not consider the uncertainties related to building and soil parameters.)

VERIFICATION OF RESPONSE MODELS

To verify the constructed analytical models, we conducted seismic-response analysis using observation records of seismographs installed on each floor of the building and confirmed that the observation records and the seismic-response analysis agreed well (Choi et al. 2017). Also, we performed an eigenvalue analysis. The results obtained from the 3D FE and SR models for the east–west direction are shown in Figure 6.

Based on the results, the natural period of the primary mode of the building was approximately 0.3 s, whereas the secondary mode was approximately 0.17 s. The primary and secondary natural periods in each model correspond. Focusing on the natural-mode shape in the 3D FE model, we confirmed that the out-of-plane deformation in the upper part of the building could not be expressed using the SR model. Similar results were obtained for the north–south direction.

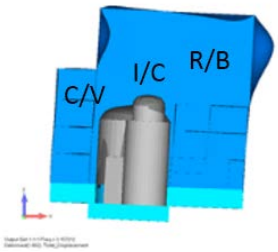

(a) First mode of 3D FE model (0.32 s).

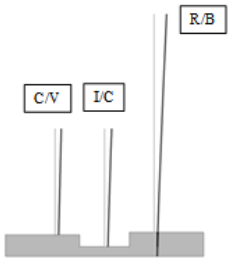

(b) First mode of embedded SR model (0.29 s).

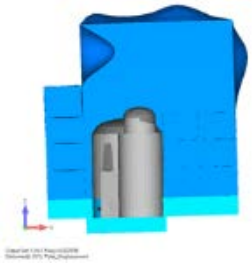

(c) Second mode of 3D FE model (0.17 s).

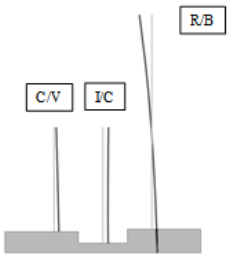

(d) Second mode of embedded SR model (0.15 s).

Figure 6. Results of eigenvalue analysis of nuclear-power-plant reactor-building models (east–west direction)

ANALYTICAL RESULTS

Results of Seismic-Response Analysis of Reactor-Building Walls

Next, we conducted seismic-response analysis of the reactor building using hazard-consistent ground motions. First, to confirm response results by the features of the input ground motion, we compared the results from two types of input ground motions (Figure 7). The time-history waveforms and response spectra of the ground motions due to the Southern Kanto Fault (input A) and fault-unspecified crustal earthquake (input B) are shown for the east–west direction for input level 1000–1100 cm/s^2 (Figures 7a and 7c). In particular, features such as the duration of the time-history waveform of the two input waves are different. The distribution of maximum-response acceleration from inputs A and B by four walls (Figure 4a) are shown in Figures 7b and 7d (lines 1C, 2C, 4C, and 4A); to compare the differences in the building modeling methods, the results of the embedded SR model are also shown. Overall, the maximum-response acceleration of the upper floors is larger for both models, and the response results of the 3D FE model tended to be larger than the results of the embedded SR model. In particular, the result for the 1C wall are significantly different due to building modeling methods. This is considered to be an effect of the out-of-plane deformation of the wall, which is a characteristic response of the 3D FE model. In contrast, the influence of the differences in the features of the input ground motion was not very large. Similar results were obtained for different input levels.

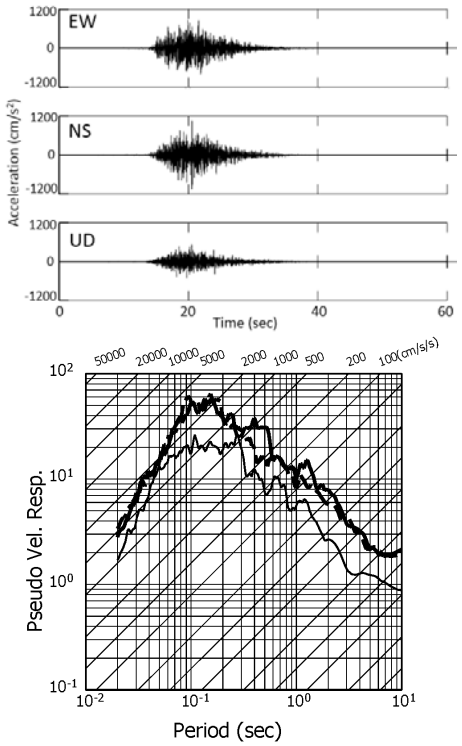

(a) Input ground motion A (Southern Kanto Fault, 1000–1100 cm/s^2).

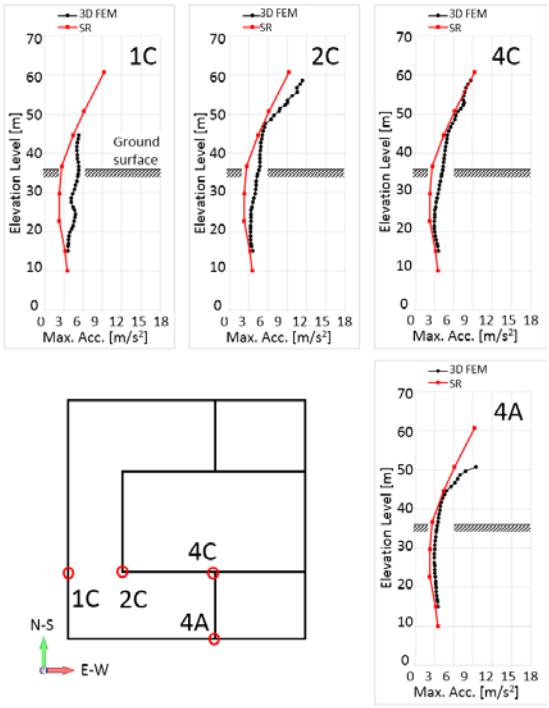

(b) Maximum-response acceleration from input A.

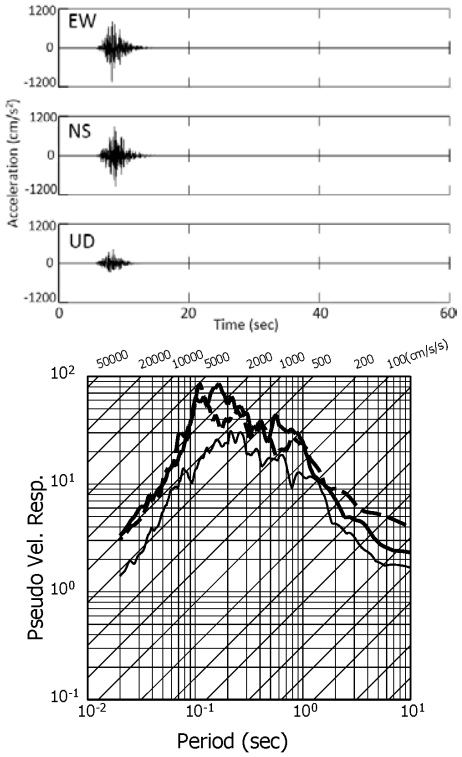

(c) Input ground motion B (crustal earthquake, 1000–1100 cm/s^2).

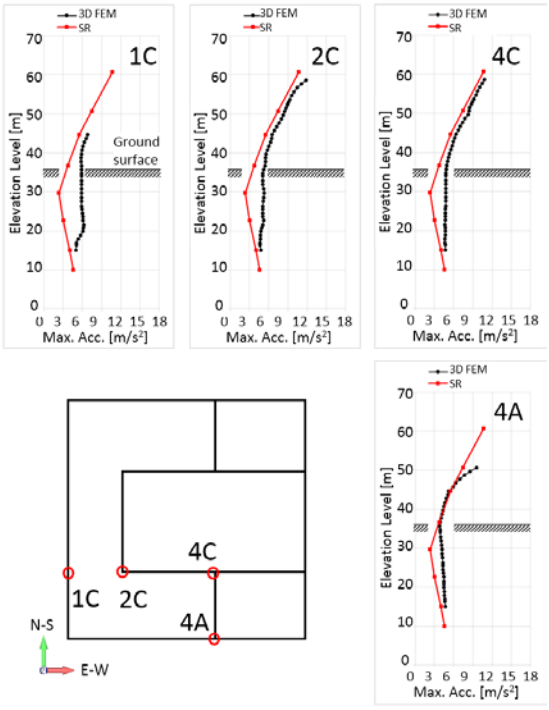

(d) Maximum-response acceleration from input B.

Figure 7. Example of maximum-response acceleration results (east–west direction).

Results of Seismic-Response Analysis Using 200 Waves

Next, we conducted seismic-response analysis of the reactor building using 200 waves of hazard-consistent ground motions. As an example, maximum-response acceleration in the horizontal (east–west direction) of the reactor building walls (4C wall) for 50 waves (input level: 1000–1100 cm/s^2), including results from both models, is shown in Figure 8. Relevant statistics of the results (the mean value and the variation as the natural-logarithm standard deviation) are shown in Figure 9. The mean of the maximum-response acceleration of the upper floors is larger for both models. Overall, the response results of the 3D FE model tended to be larger than the results of the embedded SR model. In particular, the difference between the two models was large (~20%) around first basement floor (29.7 m) and first floor (36.7 m). This is assumed to be due to the differences in the methods of modeling the SSI and 3D effects. However, the logarithm standard deviations of both the 3D FE model and the embedded SR model were almost constant regardless of the difference in height, and the mean values were both around 0.18.

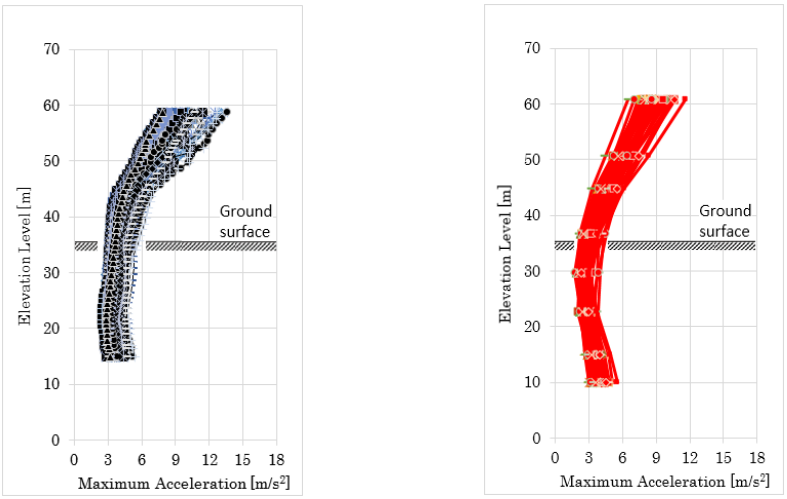

(a) Three-dimensional finite-element model (4-C wall)

(b) Embedded Sway-rocking model.

Figure 8. Example of maximum-response acceleration results (east–west direction; input level: 1000–1100 cm/s^2).

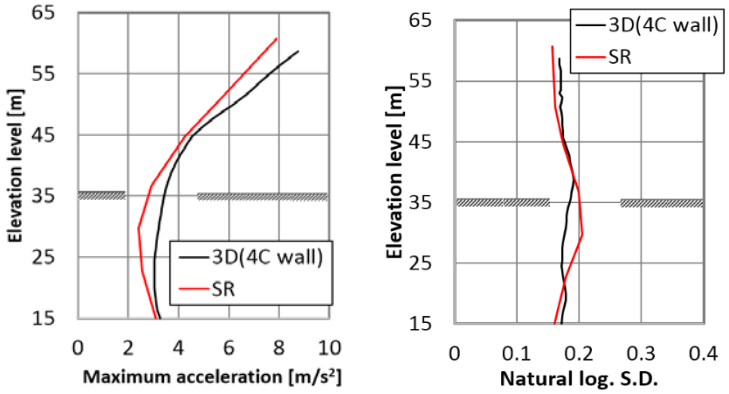

(a) Mean

(b) Standard Deviation

Figure 9. Statistics of maximum-response acceleration (east–west direction)

Influence of Input Ground-Motion Characteristics on Building Response

To confirm the influence on the building response of the characteristics of the input ground motions, we investigated the influence of different seismic sources as an example (Figure 10). We found that the influence of seismic source on building response was ~20% at the maximum.

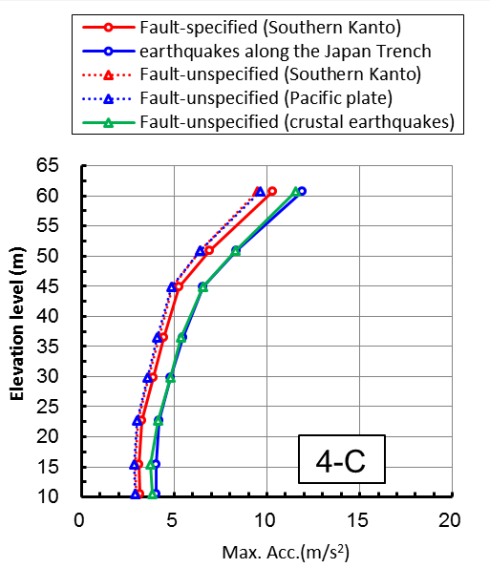

Figure 10. Mean value of maximum-response acceleration due to location of seismic sources (based on three-dimensional finite-element model, 4C wall, and east–west direction).

CONCLUSION

To clarify the influence of various ground motions on the results of the seismic-response analysis of the reactor building, we used 200 hazard-consistent ground-motion waves as input. We considered two building models, the 3D FE model and the embedded SR model, and compared the variation of building response results due to differences between the modeling methods used, with the following results:

- No significant difference was found in the seismic-response results of the two building models, in spite of using different input ground motions.
- The mean value of maximum-response acceleration of the 3D FE model tended to be larger than that of the embedded SR model. This is considered to be an effect of the out-of-plane deformation of the wall, which is a characteristic response of the 3D FE model.
- The variation of building response was about $\pm$0.2 regardless of the modeling method.
- The influence of the differences among seismic sources on the building response was ~20% at the maximum.

In the future, to contribute to the advancement of SPRAs for NPP facilities, we plan to investigate the effects of material nonlinearity, SSI, and other differences between modeling methods on the uncertainty of building response.

REFERENCES

Atomic Energy Society of Japan. (2015). "A standard for Procedure of Seismic Probabilistic Safety Assessment (PSA) for nuclear power plants 2015", (in Japanese).

Choi, B., Nishida, A., Muramatsu, K. and Takada, T. (2017). "Uncertainty evaluation of seismic response of a nuclear facility using simulated input ground motions", *Proc. 12th Int. Conf. on Structural Safety and Reliability*, Vienna, Austria.

Headquarters for earthquake research promotion (HERP). (2009). "Technical report on national seismic hazard maps for Japan" (in Japanese).

Maekawa, K. and Fukuura, N. (1999). "Re-formulation of spatially averaged RC constitutive model with quasi-orthogonal bi-directional cracking", *Journal of Materials, Concrete Structures and Pavements, JSCE*, No. 634/V-45, pp.157-176. (in Japanese).

Nishida, A., Igarashi, S., Sakamoto, S., Uchiyama, Y., Yamamoto, Y., Muramatsu, K. and Takada, T. (2015a). "Hazard-consistent ground motions generated with a stochastic fault-rupture model", *Nuclear Engineering and Design*, 295, pp.875-886.

Nishida, A., Muramatsu, K. and Takada, T. (2015b). "Seismic Response Analysis of Reactor Building and Equipment with Hazard Consistent Ground Motions Using a 3D-FE Model", *Proc., Joint International Conference on Mathematics and Computation (M&C), Supercomputing in Nuclear Applications (SNA) and the Monte Carlo (MC) Method*, Nashville, USA.

Si, H. and Midorikawa, S. (1999). "New attenuation relationships for peak ground acceleration and velocity considering effects of fault type and site condition", *J. Struct. Constr. Eng. (Transactions of AIJ)*, 523, pp.63-70. (in Japanese).

Takada, T., Itoi, T., Nishida A., Furuya, O. and Muramatsu, K. (2015). "Reliability Enhancement of Seismic Risk Assessment of NPP as Risk Management Fundamentals, Part II: Quantifying Epistemic Uncertainty in Fragility Assessment Using Expert Opinions", *Proc., SMiRT-23*, Manchester, UK.